The Three-Dimensional Distribution of Galactic AGB Stars with ALLWISE

Nicholas M. Hunt-Walker, Željko Ivezić, Andrew C. Becker

University of Washington, Department of Astronomy, Seattle, WA 98195

nmhw@uw.edu, ivezic@uw.edu, acbecker@uw.edu

1. Introduction

The structure of the Milky Way holds clues to the processes of formation and evolution of galaxies. Historical models typically assumed three discrete components described by simple analytic expressions: the thin disk, thick disk, and halo (Bahcall & Soneira 1980; Gilmore et al. 1989; Majewski 1993). Recent surveys, such as the Sloan Digital Sky Survey (SDSS, York et al. 2000) and the Two Micron All Sky Survey (2MASS, Skrutskie et al. 2006), have provided much more detail about these components. For example, SDSS data have constrained stellar distributions in the 7-dimensional space spanned by spatial coordinates (Jurić et al. 2008), velocity components (Bond et al. 2010), and metallicity (Ivezić et al. 2008). The resulting maps revealed rich, complex substructure in the distribution of the Milky Way's stars (e.g. Ivezić et al. 2000; Yanny et al. 2000; Vivas et al. 2001; Newberg et al. 2002; Majewski et al. 2003; Belokurov et al. 2006; Grillmair 2006; Vivas & Zinn 2006), deeply shaking the older view of a smooth Galaxy.

The large distance limit of about 100 kpc for some halo populations (e.g. RR Lyrae and BHB stars with SDSS, Sesar et al. 2010 and red giants with 2MASS, Majewski et al. 2003), as well as about 10 kpc for very numerous main sequence stars, is not reached when studying disk component at low galactic latitudes. As shown, for example, by Berry et al. (2012), the extinction due to interstellar dust limits the SDSS sample of main sequence stars to heliocentric distances of only a few kpc. In order to avoid detrimental effect of dust extinction, stellar samples need to be probed at longer infrared wavelengths. Several infrared surveys covering the Galactic plane have recently become available (WISE, Wright et al. 2010; Cutri et al. 2012, GLIMPSE Churchwell et al. 2009; Benjamin et al. 2003, VVV Saito et al. 2012).

Among populations suitable for studying Galactic structure using infrared surveys, Asymptotic Giant Branch (AGB) stars stand out. AGB stars represent the last stage of evolution for stars between 0.8 and 8 $M_{\odot}$ (Iben & Renzini 1983; Herwig 2005). Stars from this mass range can reach the final stages of stellar evolution within the Galactic timescale (∼10 Gyr, Iben & Renzini 1983) and thus are bound to reside throughout the Galaxy wherever other stars are present. This phase of stellar evolution is marked by two distinct episodes with different observational characteristics: the early AGB phase (E-AGB) and the thermally-pulsing AGB phase (TP). During the thermally-pulsing phase, AGB stars produce substantial dust-driven stellar winds ($10^{-7} < \dot{M} < 10^{-4}$ $M_{\odot}$ yr^{-1}, Olofsson et al. 2002) rich in oxides (SiO, Al_2O_3, etc.) or carbon-rich molecules (SiC, AmC, etc.) The dominant chemical composition is highly dependent upon the metallicity of the host

galaxy (Matsuura et al. 2005). High-metallicity galaxies like the Milky Way have a substantial population of oxygen-rich AGB stars (Habing et al. 1985), whereas low-metallicity galaxies such as the Magellanic clouds are dominated by carbon-rich AGB stars (Boyer et al. 2011). In both cases, the other species of AGB star is rarely seen, as richness in one chemical type (e.g. oxides) necessitates the almost complete capture of the other chemical type (e.g. carbon) in CO (Iben & Renzini 1983).

The dust-rich winds in TP phase create vast circumstellar shells that are warmed by the stellar photosphere and emit copiously in the near- and mid-infrared (NIR & MIR, respectively). Together with high bolometric luminosity (10^3–10^4 $M_\odot$), this redistribution of the output radiation to the infrared wavelength makes AGB stars excellent disk probe when infrared survey data are available. Indeed, they were detected all the way to the Galactic center even with the IRAS survey (Jackson et al. 2002). Such disk studies can now be significantly improved thanks to the much more sensitive WISE survey.

The *Wide-field Infrared Survey Explorer*, WISE, is a space observatory that has imaged essentially the entire sky in the MIR (3.4, 4.6, 12, and 22 μm). The WISE catalog has been positionally matched to the 2MASS catalog, with the matched catalog listing NIR and MIR 7-band photometry for hundreds of millions of sources. Given the depths of the two surveys, this catalog should contain AGB stars to many kpc beyond the Galactic center. Here we develop selection methods for AGB stars using WISE and 2MASS data, and analyse the resulting samples.

In Section 2, we describe in detail the WISE, 2MASS and other auxiliary data used in our study and the data reduction process. In Section 3, we use samples of known Galactic and Magellanic AGB stars to derive WISE-2MASS color-based selection criteria, and calibrate color-absolute magnitude relations. In Section 4, we describe the spatial density distribution of selected AGB candidates from the Milky Way. Our conclusions are summarized in Section 5.

2. Input Catalogs and Data Preparation

Our principal data source is the merged WISE-2MASS catalog. In order to derive WISE-2MASS color-based selection criteria, we use a homogenous sample of AGB stars from the OGLE-III Catalog of Variable Stars supplying objects in the Magellanic Clouds. This sample serves to calibrate color-color and color-absolute magnitude relations that underlie our distance estimates. In order to assess what infrared populations could contribute to contamination of selected AGB candidates, we utilize extragalactic sources from SDSS data release 7 pulled from the NYU Value-added Galaxy Catalog, the SDSS unofficial Luminous Red Galaxy sample, and young stellar objects obtained identified in WISE data, also described below. We conclude this section by describing how these auxiliary catalogs were positionally merged with the WISE-2MASS catalog, and summarize the object counts before and after quality control in Tables 1 & 2.

2.1. WISE-2MASS catalog

In this study, we rely heavily on data from the ALLWISE extension of the WISE survey, combining data from the initial All-Sky Data Release, the 3-band cryogenic data release, and the NEOWISE post-cryogenic data release (Cutri et al. 2013). The initial WISE All-Sky Data Release observed the sky between January and August 2010, observing the sky 1.2 times with four detectors, operating at 3.4, 4.6, 12, and 22μm. Hereon we refer to ALLWISE photometric bands at [3.4μm/4.6μm/12μm/22μm] as [$W1/W2/W3/W4$]. The positions of objects in the WISE catalog were calibrated to the 2MASS point source catalog.

The 3-band cryogenic data release contains data from $W1$, 2, and 3, and surveyed 30% of the sky between August and October 2010. During the 3-band cryogenic survey, $W1$ and $W2$ operated with nearly the same sensitivity as during the full survey. Warming of the telescope reduced sensitivity in $W3$ and fully saturated $W4$. The NEOWISE post-cryogenic data release contains $W1$ and $W2$ measurements, with sensitivities close to those obtained during the full cryogenic phase. During this phase, WISE surveyed 70% of the sky. Data products from the post-cryogenic release included updated instrumental, astrometric, and photometric calibrations and reduction algorithms, resulting in much lower SNR. The overall number of sources compiled into ALLWISE totals over 747.6 million.

2.2. AGB stars from the OGLE-III Catalog of Variable Stars

The OGLE-III Catalog of Variable Stars (CVS) (Udalski et al. 2008; Soszyński et al. 2009, 2011) is a subset of the overall OGLE-III experiment, containing roughly 10 years of observations in the V- and I-bands of over 120,000 variable stars. With high-precision photometry (0.001 mag Soszynski et al. 2007), these observations saturate at $I = 12.5$ mag, and are limited at the faint end at $I = 20.5$ mag (Zebrun et al. 2001).

The OGLE-III CVS is accessible through an online database[1], with LPVs classified by object type, evolutionary status, and spectral type. Object type is based chiefly on variability and luminosity. OGLE Small Amplitude Red Giants (hereon OSARGs) are weakly-variable ($0.005 < A_I < 0.13$ mag), with relatively short periods ($10 < P < 100$ days; Soszynski et al. 2004). Additionally, because these objects are multiperiodic, OSARGs are selected using their period ratios and their distances from established period-luminosity ($\log{}_{10}P - L$) sequences from Wood et al. (1999). For more detail in their selection, see Soszynski et al. (2007). Mira variables and Semi-Regular Variables (hereon SRVs) are identified using I-band amplitudes and $P - W_I$, where W_I is the reddening-free Wesenheit index (Soszynski et al. 2005):

$$W_I = I - 1.55(V - I) \quad (1)$$

[1] http://ogledb.astrouw.edu.pl/~ogle/CVS/

As red giant branch stars (hereon RGBs) can contaminate the same $\log_{10}P - L$ space as AGB stars, evolutionary type is distinguished in two ways. Stars above the tip of the RGB[$[I/K_s]$ = [14.56/12.05] mag in LMC (Soszynski et al. 2004, 2007)are AGBs by virtue of luminosity. Below that threshold, a narrow sequence of stars appears to share the same slope and intercept with AGB stars above the TRGB. Additionally they share similar primary-secondary period ratios as known AGB stars (Soszynski et al. 2005). However, as there is still some significant contamination by RGBs, we neglect all OGLE objects below the TRGB moving forward.

For individual $\log_{10}P-L$ sequences, spectral type (O-rich or C-rich) is easily seen as separations in $\log_{10}P - L$ space as well as visible-NIR color-color space. The initial classifications are based on spectroscopically-observed stars and were extended more generally to $\log_{10}P - L$ and visible-NIR color-color criteria (Soszynski et al. 2005, 2007). This clear separation can be seen in Figure 1.

From the initial OGLE-III sample of 52,976 LPVs, we retain 43,209 after matching to ALLWISE within 3", and ensuring only 1 match to 2MASS as well as all objects needing to be in the LMC. The I-band median of OGLE-III LPVs is $\approx$ 14.68 mag with a standard deviation of 0.72 mag. Out of the entire sample only 13 objects (Miras) fall beyond the 20.5 mag faint limit, and 41 beyond the saturation limit. As such, we expect this to effectively represent the complete sample of oscillating AGB stars in the LMC.

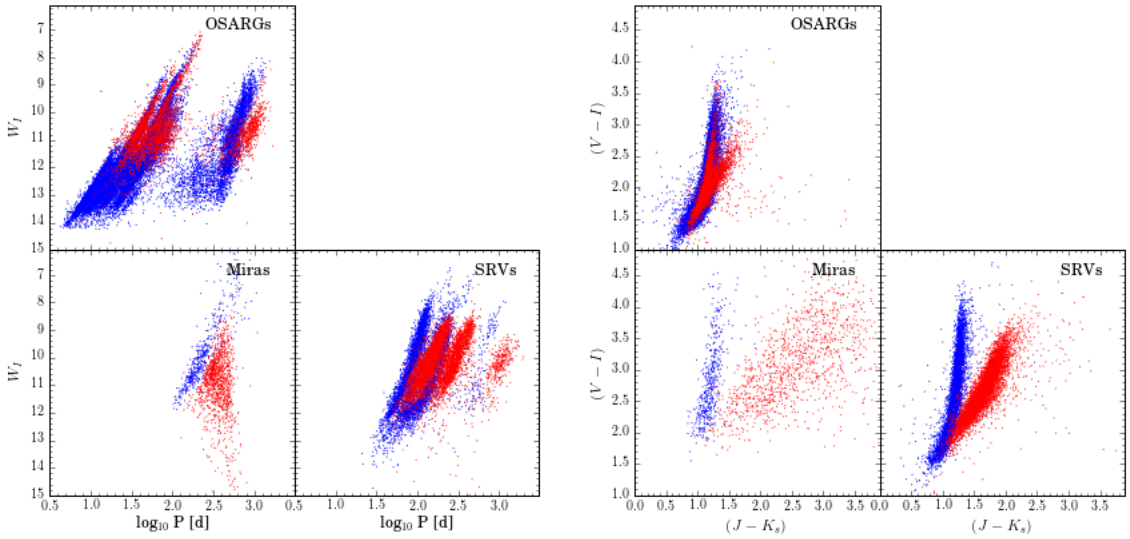

Fig. 1.— O-rich (*blue*) and C-rich (*red*) OGLE-III LPVs matched to 2MASS. *Left*: W_I vs log period in days. *Right:* OGLE-III $(V-I)$ vs 2MASS $(J-K_s)$.

2.3. Extragalactic catalogs from SDSS

SDSS is a multi-year survey of roughly 25% of the sky collecting both photometric (*u, g, r, i, z*-bands for 700+ million objects) and spectroscopic measurements (1.6+ million) of stars and extragalactic sources (York et al. 2000). Though its ground-based nature and sensitivity to interstellar extinction prevent SDSS from being an all-sky survey, it represents the largest spectrophotometric catalog to date. For this study we collect extragalactic objects from the NYU Value-added Galaxy Catalog, containing objects matched between SDSS and several auxiliary surveys spanning multiple wavelength regimes, and the unofficial SDSS Luminous Red Galaxy sample, isolating high-confidence luminous red galaxies from the SDSS database.

2.3.1. The NYU Value-added Galaxy Catalog

In order to cull the full set of SDSS spectrophotometry and produce an easily-referenced extragalactic catalog for investigating galaxy formation and evolution, the NYU Value-added Galaxy Catalog (NYU-VAGC; Blanton et al. 2005) was created as of SDSS data-release 7 (DR7).

The NYU-VAGC contains matches between SDSS spectrophotometry and the following catalogs: the FIRST radio survey, the 2MASS Point Source Catalog, the 2MASS Extended Source Catalog, the Two-degree Field Galaxy Redshift Survey, the IRAS Point Source Catalog Redshift Survey, and Reference Catalog 3 (RC3.9b). As a consequence, the NYU-VAGC retains SDSS optical photometry in addition to spectral classifications (QSO, galaxy, star) and subclassifications (AGN, starforming galaxy, starburst galaxy, etc.) for 441,707 objects across 10,417 square degrees of the SDSS footprint. Main and secondary classifications are made by comparing measured optical spectra to the SDSS spectral library. See Blanton et al. (2005) for the full set of reduction and inclusion criteria. This catalog is available via an online data repository[2], along with a full description of the data and other subsamples not used in this study. The populations for each species (QSO, AGN, starforming galaxy (SF), starburst galaxy (SB)) are found in Table 1.

2.3.2. The Unofficial Luminous Red Galaxy Sample

Subselected for the study of Baryon Acoustic Oscillations by Kazin et al. (2010), the Luminous Red Galaxy sample (LRGs; Eisenstein et al. 2001) is also sourced from SDSS DR7. LRGs contaminate the color-color space of AGB stars due to the severe redshift of their intrinsically-bright optical fluxes. We obtain the unofficial LRG sample from the data repository[3] of Kazin et al. (2010). The initial sample is volume-limited, containing 105,631 objects spanning a redshift range

[2] http://sdss.physics.nyu.edu/vagc/

[3] http://cosmo.nyu.edu/~eak306/SDSS-LRG.html

of $0.16 < z < 0.47$.

2.4. WISE+2MASS Young Stellar Objects

Young Stellar Objects (YSOs) represent a unique contaminant in our search for dust-enshrouded AGB stars. Similar to AGBs, YSOs are luminous sources surrounded by warm, dusty environments. That warm dust can then glow brightly in the MIR, easily contaminating AGB color-color space. To characterize and later eliminate this potential contaminant we select as our base sample 290 YSOs from Rebull et al. (2011), a survey searching for YSOs in the Taurus Molecular Cloud using data from WISE and ancillary data from SDSS and 2MASS. As YSO tend to be embedded within high-extinction clouds of this sort, we expect that the dust-reddened NIR/MIR emission from these objects should match to similar objects in the LMC when we later calibrate our color-color criteria.

2.5. WISE+2MASS Stellar Locus

We begin to extract the stellar locus from ALLWISE by centering on the LMC ($276.5° < l < 284°$, $-38.2° < b < -28°$) by necessitating that every object have 1 2MASS association, $[W1/W2/W3]$ signal-to-noise > 1, detections in 2MASS J, H, and K, and confusion & contamination flags set to 0 for $[W1/W2/W3]$. We then adapt the color-color criteria from Davenport et al. (2014). Their locus focuses on stars with effective temperatures $3540 < T_{\rm eff} < 7200K$. We fit their criteria for $J - K_s$ vs $W1 - W2$ within 3σ of the locus with degree-3 polynomials. The resulting fit for the 3σ stellar locus follows:

$$(J - K_s) < 61.67(W1 - W2)^3 - 17.88(W1 - W2)^2 + 1.68(W1 - W2) + 0.99 \quad (2)$$

$$(J - K_s) > 40.19(W1 - W2)^3 - 9.78(W1 - W2)^2 + 0.54(W1 - W2) + 0.64 \quad (3)$$

The resulting locus sample, as well as the original Davenport et al. (2014) bounds and locus are showin in Fig 2. Note that our sample goes beyond the limits of the stated locus.

2.6. Merged Samples

The OGLE-III AGB sample, as well as the SDSS and YSO samples, were matched to the ALLWISE data products via the `GATOR` tool at the NASA/IPAC Infrared Science Archive[4]. The accepted matching radius was 3" execept in the case of YSOs, which were limited to 1". YSO

[4] http://irsa.ipac.caltech.edu/cgi-bin/Gator/nph-scan?mission=irsa&submit=Select&projshort=WISE

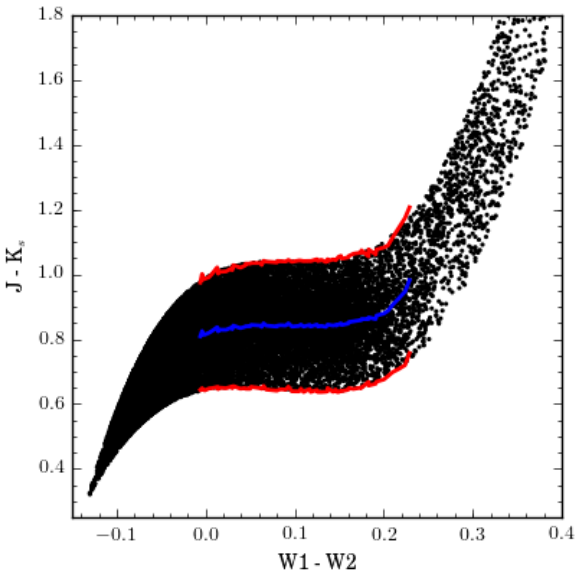

Fig. 2.— The WISE-2MASS stellar locus. (*black dots*) objects from the stellar locus in the direction of the LMC. (*blue line*) WISE-2MASS color-color stellar locus derived from Davenport et al. (2014). (*red line*) 3σ boundaries for WISE-2MASS color-color locus.

objects were obtained from the VIZIER service already possessing WISE observations, so we were able to accept a smaller matching radius as we only sought the extra 2MASS information.

The final OGLE-2MASS-WISE AGB sample is produced from the obejct sample in section 2.2. We apply the point source saturation limits of $[W1/W2/W3/K_S] < [2.0/1.5/-3.0/8.5]$. We also enforce, in order, the 5σ faint limits for $[W1/W2/W3/K_S] < [16.83/15.6/11.32/15.5]$. The WISE point source saturation and 5σ faint limits can be found in Cutri et al. (2012). The 2MASS faint and saturation limits are found in Skrutskie et al. (2006). We also enforce $[W1/W2/W3]$ SNR > 3, and contamination & confusion flags (`cc_flag`) set to 0 in each of those bands. The VAGC, LRG, and YSO samples are filtered through the same criteria. Note that we deliberately neglect $W4$ because, after applying the 5σ faint limits as well as `cc_flag`=0, our sample is too heavily reduced. The resulting populations from each reduction step can be found in Table 1.

2.7. Completeness and Contamination of the Initial AGB Sample

Sample completeness η is defined as

$$\eta = \frac{N - n_{\rm missed}}{N}$$

Population	OGLE	QSO	AGN	SF	SB	LRGs	YSOs	Locus	**Total**
Original	46,385	122,550	19,184	232,845	67,128	105,631	290	25,254	**619, 267**
WISE match	43,209	6,902	3,098	36,539	10,359	75,543	274	25,254	**201, 178**
$W1$-3, K_S saturation limit	43,201	6,900	3,098	36,538	10,358	75,527	214	25,156	**200, 992**
$W1$-2 faint limit	43,200	6,891	3,098	36,537	10,358	75,527	214	24,382	**200, 207**
$W1$-3 faint limit	19,358	6,728	3,005	35,678	10,105	1,184	214	3,154	**79, 426**
$W1$-3, K_S faint limit	19,358	5,283	2,878	34,299	9,676	1,167	213	3,070	**75, 944**
$W1$-3 SNR > 3	18,995	5,279	2,876	34,285	9,673	1,079	213	3,056	**75, 456**

Table 1: Sample populations with respect to each reduction step.

where N is the total number of objects in the sample, and $n_{\rm missed}$ is the number of objects outside of the applied boundaries. Ivezić et al. (2013) defines sample contamination as

$$\epsilon \;=\; \frac{n_{\rm spurious}}{n_{\rm selected}}.$$

where $n_{\rm spurious}$ is the number of spurious sources and $n_{\rm selected} = N + n_{\rm spurious}$.

In the next section you are using the AGB sample from this section to estimate completeness and contamination of color-selected samples. Here you need to summarize what do you believe completeness and contamination are for your initial sample constructed using SIMBAD and optical surveys. In particular, it is important to describe expected distance limits.

2.8. XXX old stuff from here to the end of this section: Data Sources

In this study, we rely heavily on data from the ALLWISE extension of the WISE survey, combining data from the initial All-Sky Data Release, the 3-band cryogenic data release, and the NEOWISE post-cryogenic data release (Cutri et al. 2013). The initial WISE All-Sky Data Release observed the sky between January and August 2010, observing the sky 1.2 times with four detectors, operating at 3.4, 4.6, 12, and 22μm. Hereon we refer to ALLWISE photometric bands at [3.4μm/4.6μm/12μm/22μm] as [$W1/W2/W3/W4$]. The positions of objects in the WISE catalog were calibrated to the 2MASS point source catalog. The 3-band cryogenic data release contains data from $W1$, 2, and 3, and surveyed 30% of the sky between August and October 2010. During the 3-band cryogenic survey, $W1$ and $W2$ operated with nearly the same sensitivity as during the full survey. Warming of the telescope reduced sensitivity in $W3$ and fully saturated $W4$. The NEOWISE post-cryogenic data release contains $W1$ and $W2$ measurements, with sensitivities close to those obtained during the full cryogenic phase. During this phase, WISE surveyed 70% of the sky. Data products from the post-cryogenic release included updated instrumental, astrometric, and photometric calibrations and reduction algorithms, resulting in much lower SNR. The overall number of sources compiled into ALLWISE totals over 747.6 million.

In order to generate a reliable, high-confidence catalog of Galactic candidate AGB stars, we

must first define color-color criteria from known AGB star samples. We select AGB stars from three source catalogs: the *Optical Gravitational Lens Experiment-III Variable Star Catalog* (OGLE-III, Udalski et al. 2008; Soszyński et al. 2009, 2011), the *MAssive Compact Halo Objects* project (MACHO, Alcock et al. 1997), and the SIMBAD Astronomical Database (Wenger et al. 2000).

OGLE-III photometry for Long-Period Variables (LPVs) in the Small and Large Magellanic Clouds (SMC and LMC respsectively) was obtained between July 2001 and May 2009, with stars in the central 4.5-deg^2 of the LMC and SMC having an additional 5 observing seasons of photometry from OGLE-II. LPVs were classified into 3 categories: OGLE-III Small Amplitude Red Giants (OSARGs), Semi-Regular Variables (SRVs), and Miras. All AGB stars O-rich and C-rich AGB stars in OGLE-III were photometrically selected using reddening-free Wesenheit magnitudes, described in detail in Soszyński et al. (2009, 2011). [Describe the selection bit in a little more detail, along with their sample completeness, selection biases, and contamination fractions] Data reduction techniques are described in Udalski et al. (2008). The resulting samples yield 46,467 AGB stars from the LMC (37,203 O-rich; 9,264 C-rich) and 6,509 stars from the SMC (3,727 O-rich; 2,782 C-rich).

From MACHO we obtain the sample of SMC, LMC, and Galactic Bulge AGB stars used in Fraser et al. (2008) (14,861 stars). Why were these objects selected? Howe were they selected? What is their completeness, selection bias, and contamination fraction? Following Fraser et al. (2008), the objects are divided into sequences (seq) 1-4. Sequence 1 primarily contains Mira variables pulsating in their fundamental modes, whereas Sequences 2-4 contain semi-regular variables in various pulsation modes.

The sample of AGB stars from SIMBAD was obtained by querying all objects classified as C-stars (18,656), S-stars (1,108), OH/IR stars (825), AGB stars (2,359), and Mira variables (9,608), for a total of 32,556 stars. Objects are classified spectroscopically, though by a variety of methods owing to the heterogeneous data housed within SIMBAD. Together with MACHO and OGLE-III, the total sample of AGB stars is 100,393. Because there is a high likelihood that samples between OGLE-III, MACHO, and SIMBADoverlap, we retain only unique objects after the initial data reduction in section 2.9.

We use SDSS spectroscopic catalogs to find and quantify regions in NIR-MIR color-color space populated by plausible contaminant sources. These include any Galactic stellar objects and planetary nebulae, as well as a host of extragalactic sources. Data for active galactic nuclei (AGN; 19,184 objects), quasi-stellar objects (QSOs; 122,550 objects), and star forming/burst galaxies (820,272 objects total) were drawn from SDSS DR7, specifically from the NYU Value Added Galaxy Catalog[5] (Blanton et al. 2005, VAGC). Luminous Red Galaxies (LRGs) were selected from the SDSS Luminous Red Galaxy Survey (105,631 objects, Kazin et al. 2010). Data for stars in the SDSS stellar locus were drawn from the DR 9 SEGUE Stellar Parameters Pipeline (SSPP) (1,843,190 objects, Ahn et al. 2012). Include bit about YSOs and PNe from SIMBAD

[5] http://sdss.physics.nyu.edu/vagc/

2.9. Data Reduction

We use NASA/IPAC IRSA's GATOR tool[6] to positionally match SDSS, OGLE-III, MACHO, and SIMBAD to ALLWISE. We select only matches within 3" between each sample and ALLWISE. All samples of AGB were required to be brighter than the published 5σ faint limits of [16.83/15.6/11.32/8.0], as well as fainter than the saturation limits of [2.0/1.5/-3.0/-4.0] extrapolated from the wings of the PSFs for point sources, for $[W1/W2/W3/W4]$ (Cutri et al. 2013), with no flags for confusion or contamination as a spurious source in any band. We also require only single associations with 2MASS objects within 3", detections in $[J/K_S/W1/W2/W3/W4]$, and SNR > 3 in each ALLWISE band.

The population for each sample from initial matching as well as after the application of the ALLWISE faint limits, saturation limits, and 2MASS detection requirements are shown in Table 2. The WISE color-color distributions for the AGB and contaminant samples are shown in Figure 3.

Population	SIMBAD AGB*	C*	Mira	OH/IR	S*
3" match	1,689	14,209	9,027	406	1,081
Reduced	684	1,782	3,241	43	511
Population	MACHO seq1	seq2	seq3	seq4	
3" match	5,279	3,519	2,619	3,070	
Reduced	277	185	73	61	
Population	OGLE-III C-rich	O-rich			
3" match	11,542	38,848			
Reduced	249	730			
Population	DR12 SSPP	DR7 LRG	QSO	AGN	Galaxies
3" match	1,578,329	104,345	103,590	18,528	841,712
Reduced	67,508	84	3,977	1,069	44,314

Table 2: AGB and contaminant populations matched to WISE before and after sample reduction in section 2.9. MACHO sequences (seq1-seq4) are from Fraser et al. (2008) and described briefly in section 2.8.

3. Object Selection Criteria

In creating color-color criteria to generate a catalog of AGB candidates, we seek to maximize AGB completeness while minimizing contamination from non-AGB objects to beneath the 1% level.

[6] http://irsa.ipac.caltech.edu/cgi-bin/Gator/nph-scan?mission=irsa&submit=Select&projshort=WISE

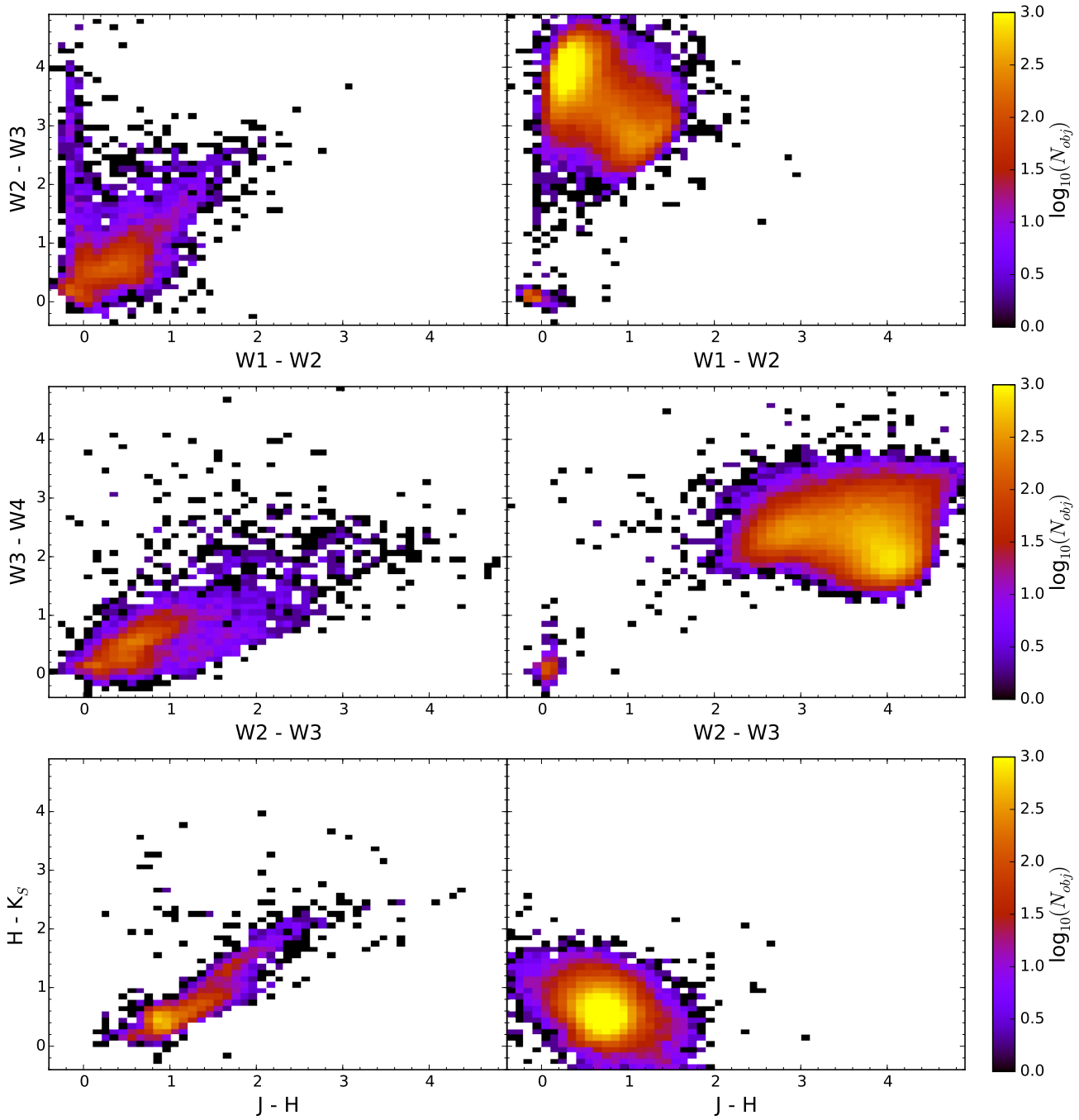

Fig. 3.— Logarithmic number densities for objects in WISE and 2MASS color-color space, binned in 0.1 dex on each axis. *Left:* The combined AGB sample matched to ALLWISE. *Right:* The combined contaminant sample.

The color-color criteria for AGB selection are as follows:

$$(J - K_s) > 1.1 \tag{4}$$

$$(W2 - W3) > 0.3 \tag{5}$$

$$(W3 - W4) < -0.83(W2 - W3) + 3.37 \tag{6}$$

The criteria in (4) and (5) are primarily concerned with rejecting objects from the stellar locus, and other objects whose NIR spectra are dominated by the Rayleigh-Jeans tail. (6) also rejects stars from the stellar locus, but primarily functions to remove IR-bright extragalactic sources.

We also experiment with other criteria to focus more closely on the high-reliability AGB population, instead of trying to capture the most AGB-like objects. These criteria are as follows:

$$(W1 - W2) < 1 \tag{7}$$

$$(W2 - W3) < 1 \tag{8}$$

Criteria (**??**) restricts NIR excesses. Criteria (8) primarily removes extragalactic sources, while only slightly cutting into the distribution of known AGB stars.

Sample completeness η is defined as

$$\eta = \frac{N - n_{\rm missed}}{N}$$

where N is the total number of objects in the sample, and $n_{\rm missed}$ is the number of objects outside of the applied boundaries. Figure 4 shows the distribution of sample completeness amongst AGB sources after the application of the above criteria. The vast majority (79.07%) of Galactic AGB stars is recovered after criteria (4), (5), and (6) are applied. The largest losses occur at the edges of the Galactic disk ($|b| \approx 10°$) and in regions of high stellar number density both in the Galaxy and the Magellanic Clouds. In the color-color diagrams, selection completeness degrades near the borders of the selection area, as objects that straddle these boundaries may exhibit enough emission in other color-color spaces to be removed by our criteria. Of the remaining sample of 5,709 objects, 52.94% lie within the disk ($|b| < 10°$).

Ivezić et al. (2013) defines sample contamination as

$$\epsilon = \frac{n_{\rm spurious}}{n_{\rm selected}}.$$

where $n_{\rm spurious}$ is the number of spurious sources and $n_{\rm selected} = N + n_{\rm spurious}$. The contamination map is shown in Figure 5. Most bins in Figure 5 exhibit 0% contamination, with the overall contamination level at 0.38%. What contaminants do remain exist primarily at the very fringes of the AGB star distribution in $(J - K_S)$ vs $(W2 - W3)$ space and near the redder boundary in $(W3 - W4)$ vs $(W2 - W3)$, where bluer extragalactic sources creep into the selection region. The results of the applied criteria on both the collective AGB and contaminant samples are summarized in Table 4.

Table 3: Samples Recovered wih Application of Criteria (%)

Object Type	Reduced	(1)	(2)	(3)	(1,2)	(1,2,3)	—	**(4)**	**(5)**	**(1,2,4)**	**(1,2,5)**	**(1,2,4,5)**
All AGBs	7220	95.15	84.89	95.21	82.62	79.07	—	**94.22**	**88.82**	**77.05**	**72.71**	**71.14**
O-rich AGB	3147	98.98	100.00	100.00	98.98	98.98	—	**98.44**	**97.33**	**97.43**	**96.31**	**94.88**
C-rich AGB	540	99.26	99.81	99.26	99.07	98.33	—	**57.59**	**63.33**	**56.85**	**62.59**	**54.44**
Unclassed AGB	3533	91.11	69.15	90.32	65.53	58.39	—	**96.07**	**85.14**	**61.99**	**53.24**	**52.53**
DR12 SSPP	67508	76.16	99.16	0.91	76.07	0.05	—	**86.05**	**0.89**	**65.67**	**0.03**	**0.03**
DR7 LRG	84	96.43	100.00	0.00	96.43	0.00	—	**89.29**	**0.00**	**85.71**	**0.00**	**0.00**
QSO	3783	73.54	99.97	0.13	73.54	0.11	—	**34.50**	**0.11**	**27.54**	**0.08**	**0.08**
Galaxy	42066	78.55	100.00	0.01	78.54	0.00	—	**96.39**	**0.01**	**75.31**	**0.00**	**0.00**
AGN	1011	79.33	100.00	0.00	79.33	0.00	—	**96.34**	**0.00**	**75.87**	**0.00**	**0.00**

We note that while we do achieve a low rate of contamination, most of our contaminant sources are out of the plane of the Galaxy, while many of our AGB sources are within the Galactic disk. Considering how our extragalactic contaminant sources are from various iterations of SDSS, we know that their spatial distributions should be effectively uniform across the sky [cite me]. For contaminants unaffected by interstellar reddening, they would occupy the same regions of color-color space already marked by our existing contaminant sample, and would similarly be removed by (4), (5), and (6). This would produce the same zero-level contamination for all extragalactic sources aside from QSOs. We can adopt a QSO spatial density by dividing the total number of spectroscopically identified QSOs by the covered area on the sky. Using this, we recover a QSO spatial density of some number per square degree. Using that density, and assuming ubiquity of sources on the sky, complete detection of QSOs down to some magnitude limit, and a lack of interstellar reddening, we can estimate a maximum QSO contamination fraction of some number. We use this number to report our QSO contamination fraction in Table 4, as QSOs significantly affected by interstellar reddening would exist further outside of the limits of (4), (5), and (6). A more rigorous study of QSO spatial density is outside the scope of this paper.

The remaining contaminant sample is from the SDSS DR12 SSPP, with the number of remaining species found within shown in Figure 6. the figures don't match up with each other. The number of red stars on the right side of the fig are significantly less than those in the histogram. Reconcile this.

4. AGB Candidate Distribution

Put words here

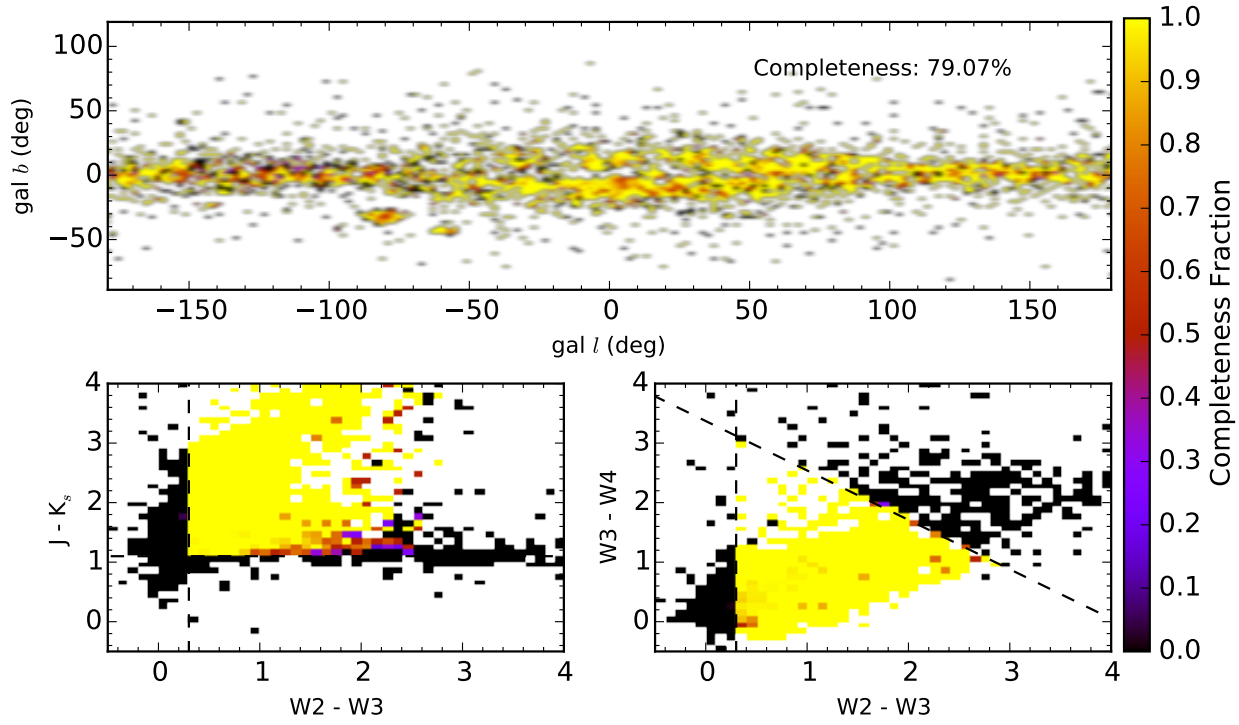

Fig. 4.— Sample selection completeness maps in (l, b) space (*top*) and the color-color space of our selection criteria (*bottom*). Color scale shows the completeness fraction per bin, with 4-deg^2 bins on the Galactic map and 0.1 dex bins on each axis of the color-color diagrams. Selection criteria are shown as dashed lines.

5. Conclusions

Put words here

REFERENCES

Ahn, C. P., et al. 2012, *Ap. J. Suppl.*, 203, 21

Alcock, C., et al. 1997, *Ap. J.*, 482, 89

Bahcall, J. N., & Soneira, R. M. 1980, *Ap. J. Suppl.*, 44, 73

Belokurov, V., et al. 2006, *Ap. J. (Letters)*, 642, L137

Benjamin, R. A., et al. 2003, *Pub. A.S.P.*, 115, 953

Berry, M., et al. 2012, *Ap. J.*, 757, 166

Blanton, M. R., et al. 2005, *A. J.*, 129, 2562

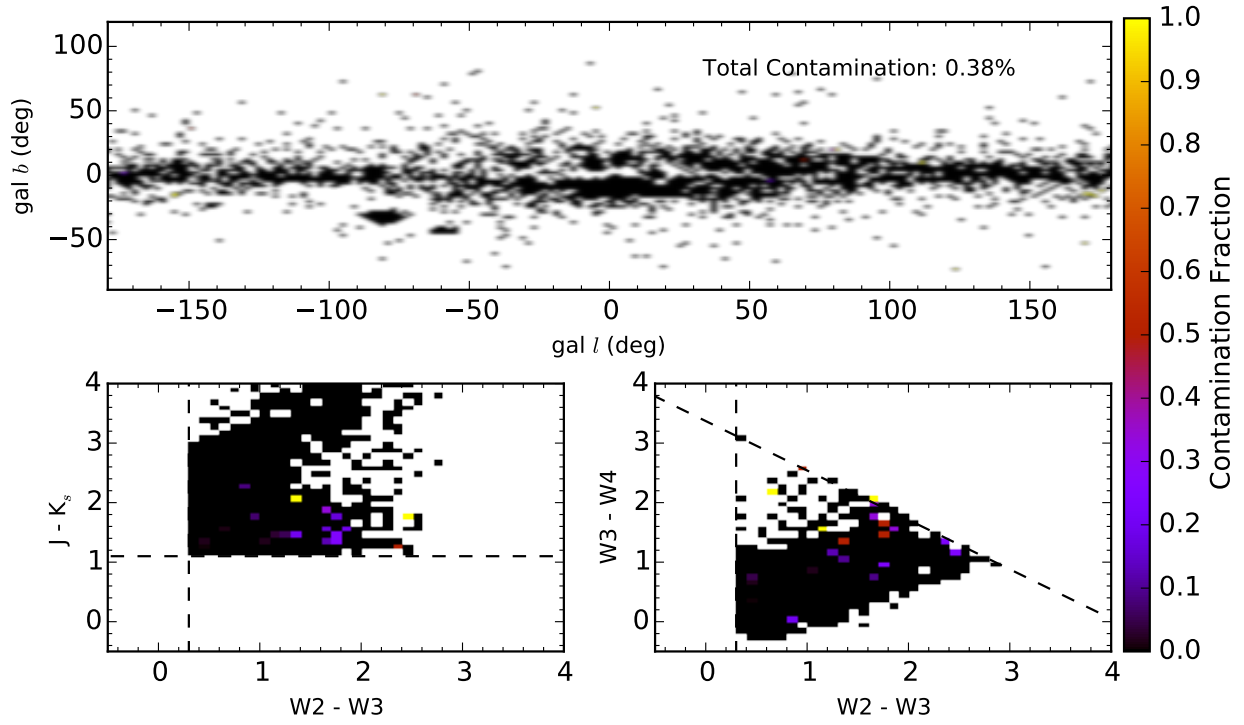

Fig. 5.— Sample contamination in Galactic (l, b) space (*top*) and color-color space (*bottom*). Boundaries and binning the same as Fig 4.

Bond, N. A., et al. 2010, *Ap. J.*, 716, 1

Boyer, M. L., et al. 2011, *A. J.*, 142, 103

Churchwell, E., et al. 2009, *Pub. A.S.P.*, 121, 213

Cutri, R. M., et al. 2012, Explanatory Supplement to the WISE All-Sky Data Release Products, Tech. rep.

—. 2013, Explanatory Supplement to the AllWISE Data Release Products, Tech. rep.

Davenport, J. R. A., et al. 2014, *M.N.R.A.S.*, 440, 3430

Eisenstein, D. J., et al. 2001, *A. J.*, 122, 2267

Fraser, O. J., Hawley, S. L., & Cook, K. H. 2008, *A. J.*, 136, 1242

Gilmore, G., Wyse, R. F. G., & Kuijken, K. 1989, *Ann. Rev. Astr. Ap.*, 27, 555

Grillmair, C. J. 2006, *Ap. J. (Letters)*, 651, L29

Habing, H. J., Olnon, F. M., Chester, T., Gillett, F., & Rowan-Robinson, M. 1985, *Astr. Ap.*, 152, L1

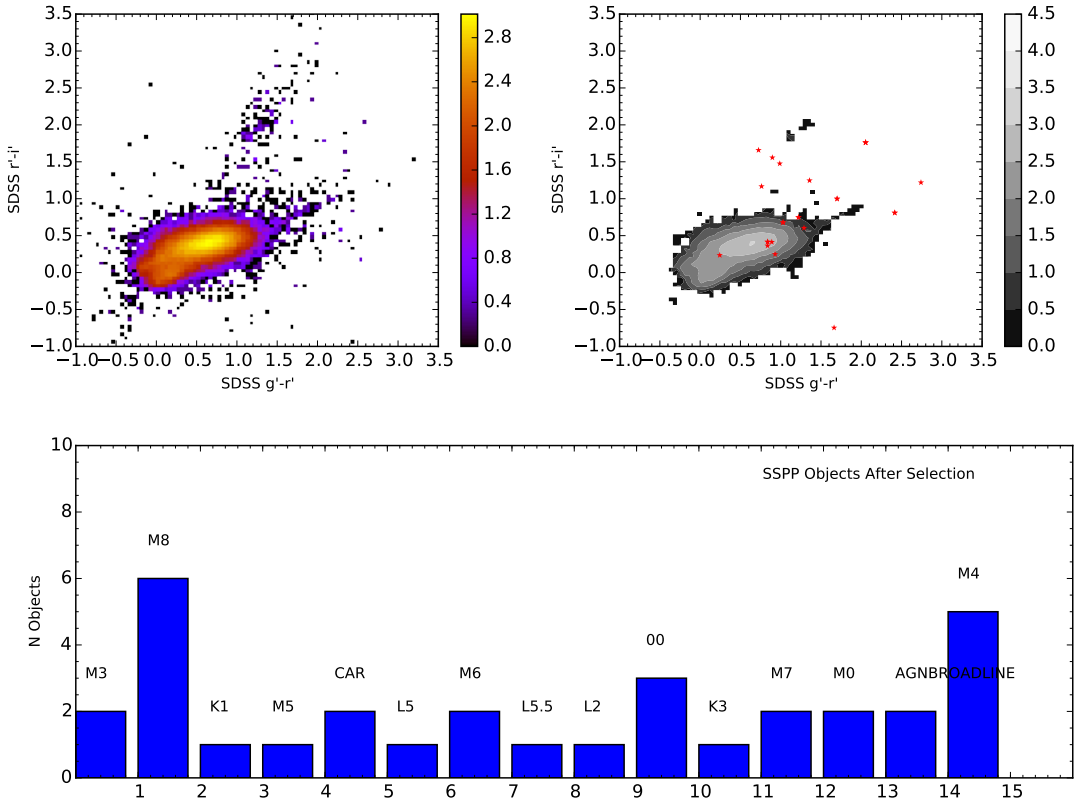

Fig. 6.— Some histogram

Herwig, F. 2005, *Ann. Rev. Astr. Ap.*, 43, 435

Iben, Jr., I., & Renzini, A. 1983, *Ann. Rev. Astr. Ap.*, 21, 271

Ivezić, Ż., Connolly, A., VanderPlas, J., & Gray, A. 2013, Statistics, Data Mining, and Machine Learning in Astronomy

Ivezić, Ž., et al. 2000, *A. J.*, 120, 963

—. 2008, *Ap. J.*, 684, 287

Jackson, T., Ivezić, Ž., & Knapp, G. R. 2002, *M.N.R.A.S.*, 337, 749

Jurić, M., et al. 2008, *Ap. J.*, 673, 864

Kazin, E. A., et al. 2010, *Ap. J.*, 710, 1444

Majewski, S. R. 1993, *Ann. Rev. Astr. Ap.*, 31, 575

Majewski, S. R., Skrutskie, M. F., Weinberg, M. D., & Ostheimer, J. C. 2003, *Ap. J.*, 599, 1082

Table 4: Sample Selection Completeness and Contamination

Population	SIMBAD AGB*	C*	Mira	OH/IR	S*
Completeness	89.62%	72.11%	95.62%	39.53%	22.31%
Population	MACHO seq1	seq2	seq3	seq4	
Completeness	88.45%	81.08%	28.77%	14.75%	
Population	OGLE-III C-rich	O-rich	**All AGB Stars**		
Completeness	73.09%	70.68%	**79.07%**		
Population	DR12 SSPP	DR7 LRG	Galaxies	QSO	AGN
Contamination	0.56%	0.00%	0.00%	0.07%	0.00%

Matsuura, M., et al. 2005, *Astr. Ap.*, 434, 691

Newberg, H. J., et al. 2002, *Ap. J.*, 569, 245

Olofsson, H., González Delgado, D., Kerschbaum, F., & Schöier, F. L. 2002, *Astr. Ap.*, 391, 1053

Rebull, L. M., et al. 2011, *Ap. J. Suppl.*, 196, 4

Saito, R. K., et al. 2012, *Astr. Ap.*, 537, A107

Sesar, B., et al. 2010, *Ap. J.*, 708, 717

Skrutskie, M. F., et al. 2006, *A. J.*, 131, 1163

Soszynski, I., et al. 2007, *Acta Astronomica*, 57, 201

Soszynski, I., Udalski, A., Kubiak, M., Szymanski, M., Pietrzynski, G., Zebrun, K., Szewczyk, O., & Wyrzykowski, L. 2004, *Acta Astronomica*, 54, 129

Soszynski, I., et al. 2005, *Acta Astronomica*, 55, 331

Soszyński, I., et al. 2009, *Acta Astronomica*, 59, 239

—. 2011, *Acta Astronomica*, 61, 217

Udalski, A., Szymanski, M. K., Soszynski, I., & Poleski, R. 2008, *Acta Astronomica*, 58, 69

Vivas, A. K., & Zinn, R. 2006, *A. J.*, 132, 714

Vivas, A. K., et al. 2001, *Ap. J. (Letters)*, 554, L33

Wenger, M., et al. 2000, *Astr. Ap. Suppl.*, 143, 9

Wood, P. R., et al. 1999, in IAU Symposium, Vol. 191, Asymptotic Giant Branch Stars, ed. T. Le Bertre, A. Lebre, & C. Waelkens, 151

Wright, E. L., et al. 2010, *A. J.*, 140, 1868

Yanny, B., et al. 2000, *Ap. J.*, 540, 825

York, D. G., et al. 2000, *A. J.*, 120, 1579

Zebrun, K., Soszynski, I., & Wozniak, P. R. 2001, *Acta Astronomica*, 51, 303